Proceedings of the 17th International Heat Transfer Conference, IHTC-17
14 – 18 August 2023, Cape Town, South Africa
IHTC-17 | ID: 294

Performance investigation on different form factor embedded heat pipe and pulsating heat pipe heat spreaders

Sai Kiran Hota[1*], Kuan-Lin Lee[1], Greg Hoeschele[1], Richard W. Bonner[1], Srujan Rokkam [1]

[1]Advanced Cooling Technologies, Inc. Lancaster, PA. 17601, USA

ABSTRACT

Addressing the thermal management challenge of high-performing power electronics is imperative for standardization. While the performance of a conduction plate heat spreader is limited, passive heat spreading alternatives like Embedded Heat Pipes (EHP) and Pulsating Heat Pipes (PHP) can spread heat more effectively and handle higher heat flux. In this manuscript, the thermal performance of two different form factor heat spreaders was compared experimentally at operating temperatures of 20 °C and 40 °C. The EHP was essentially copper-water heat pipes embedded into an aluminum base plate. The PHPs had internal capillary channels of size 1.6 mm. Testing results indicated that the PHP was more susceptible to dry-out compared to the EHP, where no dry-out was observed. PHP showed comparable or lower thermal resistance than the EHP at lower heater powers when the operating temperature was 20 °C. In all other cases, EHP demonstrated lower thermal resistance than the PHP.

KEY WORDS: Thermal management, Two-phase cooling, heat transfer enhancement, electronics cooling, pulsating heat pipe, heat pipe

1. INTRODUCTION

Recent advances and miniaturization of semiconductor devices have resulted in the growth of high-performance and high-power density electronics. However, these advancements have also led to increased heat flux dissipation and electronics temperature which could hinder the efficiency and the life of electronics [1]. In general, electronic chip temperature must be maintained below 75 °C [2]. The thermal management challenge must be addressed for the reliable operation of these electronic chips and to aid in the deployment of standardized high-power electronics across various applications. Heat spreaders are used to spread and transfer heat from these small electronics to the heat sinks. Existing commercial heat spreaders are conduction based, like aluminum plates. The performance of aluminum plates is not satisfactory for high heat flux applications due to limited thermal conductivity of 200 W/m-K. As an alternative to conduction cooling, mini/ micro-channel cooling options have been explored. Although the thermal performance is higher than conduction plate [3], there is usually a penalty of pumping power associated with the fluid circulation. Recently, passive heat spreading devices based on Embedded Heat Pipes (EHP) and pulsating heat pipes (PHP) have gained more attention as a superior alternative to the conduction heat spreader and pumped fluid microchannel heat spreader.

EHPs and PHPs are passive heat spreaders, utilizing saturated two-phase working fluid to spread heat from local hot spots to heat sinks. The operation mechanism of the regular heat pipes is as follows [4]: the heat transferred at the evaporator (chips) causes the working fluid to vaporize at the wick surface. The vapor carrying latent heat then transports to the condenser (heat sink), where the fluid condenses. The liquid then returns through the wick structure by means of the capillary action. On the other hands, the operation mechanism of PHP is as follows [5]: the working fluid randomly distributes into liquid slugs and vapor plugs in the capillary channels. When heat is added, the heat causes vaporization of the liquid slug in the vicinity of the evaporator causing the vapor pressure to increase. This pushes the adjacent liquid slug towards the condenser, where the vapor shrinks or collapses thereby causing the vapor pressure to decrease.

* Corresponding author: saikiran.hota@1-act.com

During quasi-steady state operation, these activities are simultaneously occurring, so this results in oscillation/ pulsation of the working fluid while transporting heat from the evaporator to the condenser.

Heat pipes are well understood technologies since its advent in the 1960's. As such heat spreaders with EHP have been vastly explored receiving much commercial success in recent years. On the other hand, PHPs are a more recent invention and is gaining attention as an alternative to heat pipe-based passive thermal management option. Published literature has mostly demonstrated and discussed applications of these passive two-phase heat spreaders technologies independently [6, 7, 8, 9]. One of the recent publications draws a performance comparison between EHP heat spreader-based electronics module and the PHP heat spreader-based electronics module in an enclosed chassis [10]. In this paper, performance comparison of the two-passive heat spreaders- EHP and PHP is presented for two different standard form factor sizes as defined by ANSI VITA 48.2 standards [11]. The specifications of the heat spreaders and experimental methodology is described in the section 2. The comparative thermal performance of the heat spreaders is shown in section 3. Then finally conclusion is provided.

2. HEAT SPREADER DESCRIPTION AND EXPERIMENTAL PROCEDURE

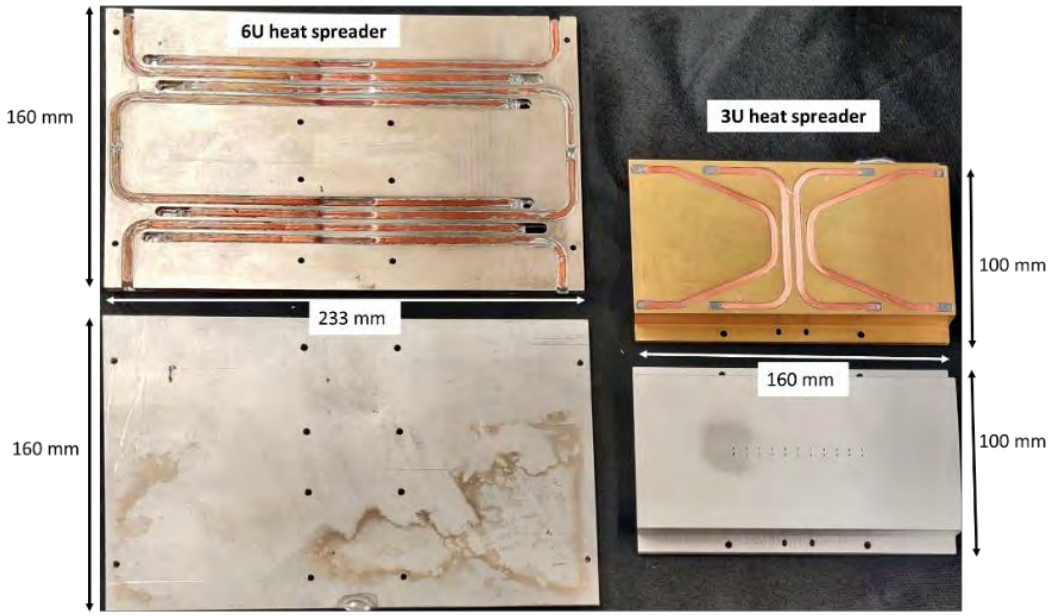

Figure 1. Two-phase heat spreaders used for performance comparison (upper row: EHP plate, lower row PHP plate)

The EHP and PHP heat spreaders were fabricated for experimental performance testing in two different form factors. The mechanical specifications of the heat spreaders are described in Table 1 and shown in Figure 1. The mechanical sizes for 6U and 3U conform to ANSI/VITA 48.2 standards [11]. The 6U form factor heat spreaders were essentially flat plate in nature. In the 6U-EHP, 8 copper-water heat pipes were embedded into the base plate in a symmetrical manner. The 6U-PHP was fabricated by means of vacuum brazing a grooved aluminum plate. The 3U form factor heat spreader consisted of a step turn to interface with a card retainer (programmatic requirements). In the 3U-EHP, 4 copper-water heat pipes were embedded onto the base plate. The heat pipes were embedded on 2D plane and could not be incorporated into the stepped plane due to fabrication limitations. So, the heat transfer along the stepped plane EHP is by material conduction. The 3U-PHP was fabricated by additive manufacturing method with aluminum. The fluid channels in the PHP could be incorporated into the stepped plane.

Table 1. Mechanical specifications of the form factor heat spreaders and test components [11]

Form factor standard	6U	3U
Length (mm)	233	100
Width (mm)	160	160
Thickness (mm)	3.56	3.38

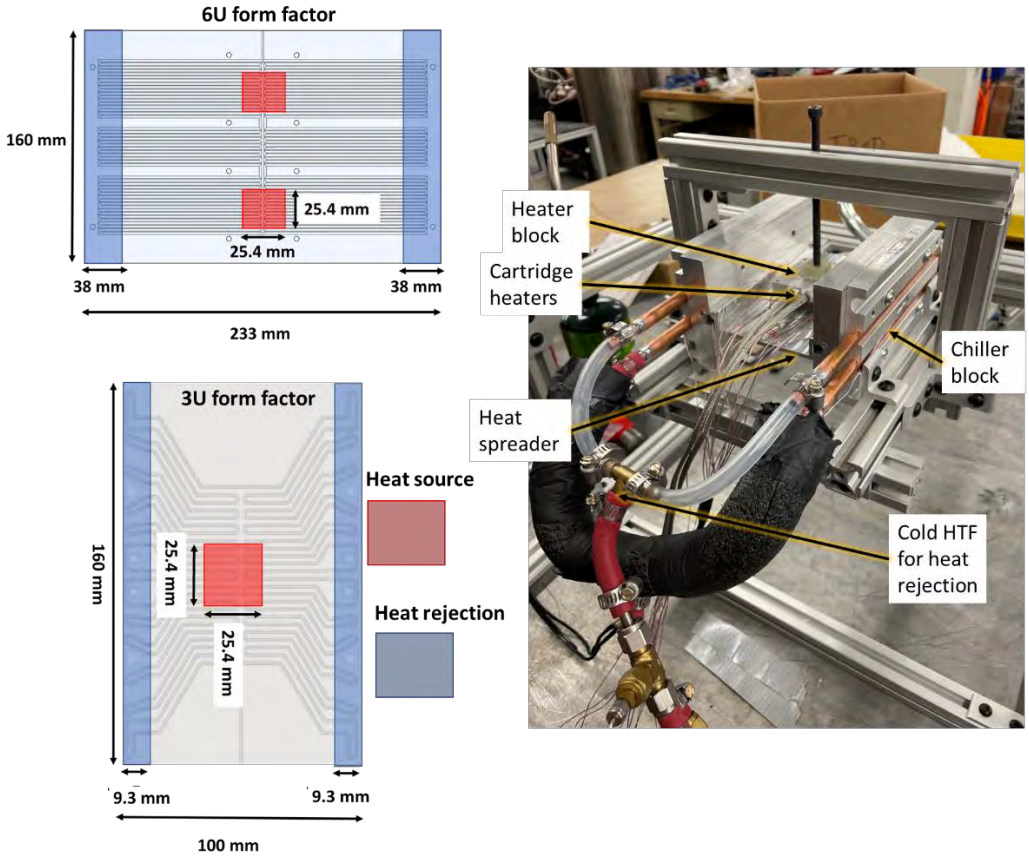

Figure 2. PHP channel layout along (left) and Experimental system for performance testing of the heat spreaders (3U heat spreader is shown)

Figure 2 shows the PHP channels layout along with the heater and the experimental test setup. A central heater and edge heat rejection configuration was chosen for performance testing. A 25.4 mm x 25.4 mm aluminum block with cartridge rod inserts was used as the heat source. A cold plate with coolant flowing at constant temperature was used for heat rejection. In the 6U form factor, the cold plate was directly in contact with the heat rejection portion of the heat spreader. In the 3U form factor, the cold plate was attached to the heat spreader via a card retainer. ICE-Lok® [1]. So, the heat rejection in the 3U form factor heat spreader was over a smaller width of 9.3 mm.

[1] https://www.1-act.com/products/ice-lok-thermally-enhanced-wedgelock/

For heat spreader performance testing, quasi-steady state method was adopted with incremental heater power and constant heat sink temperature. The testing was performed either until the maximum heat spreader temperature of 70 °C or when dry-out occurred in the heat spreader. Performance testing was done by maintaining the cold plate at constant temperatures of 20 °C, and 40 °C, which will be referred to as the heat sink (operating) temperature. The measured thermal resistance of the heat spreader was calculated as:

$$R = \frac{\Delta T}{Q} \tag{1}$$

Where, R is the thermal resistance, ΔT is the average temperature difference between the average evaporator temperature (T_e) and the average condenser temperature (T_e), and Q is the heater power. The thermocouples on the evaporator were located next to the heater block. The condenser thermocouples on the 6U heat spreaders were placed on the heat spreader below the cold plate and on the 3U heat spreaders were placed next to the card retainer. In the case of the 6U heat spreader, there were two evaporators and two edge condensers forming four evaporator-condenser pairs. So, the effective heater power was total power divided by 4. Likewise, in the 3U heat spreader, there was one evaporator and two edge condensers forming two evaporator-condenser pairs. So, the effective heater power was total power divided by 2. Testing was performed in the horizontal orientation after insulating the system with a 1-inch thick insulation foam.

Data uncertainty was measured as:

$$U = \sqrt{\left(\frac{\delta Q}{Q}\right)^2 + \left(\frac{\delta T_c}{\Delta T}\right)^2 + \left(\frac{\delta T_e}{\Delta T}\right)^2} \tag{2}$$

The measurement accuracy of the heater was ±5 W and thermocouple accuracy was ±0.25 °C. The maximum uncertainty at for 6U EHP heat was calculated to be 3.67%, and for 3U PHP was 3.3%.

3. EXPERIMENTAL RESULTS

3.1 Establishing Baseline thermal performance of the heat spreaders

Firstly, the thermal performance of the baseline plate was established for two-phase heat spreaders performance comparison. Empty PHP was used as the baseline for both 3U and 6U heat spreaders. The empty PHP plate was mounted on the test fixture for performance testing at 20 °C and 40 °C operating temperatures. For brevity, only the wall temperature profile of the heat spreader at 20 °C is shown.

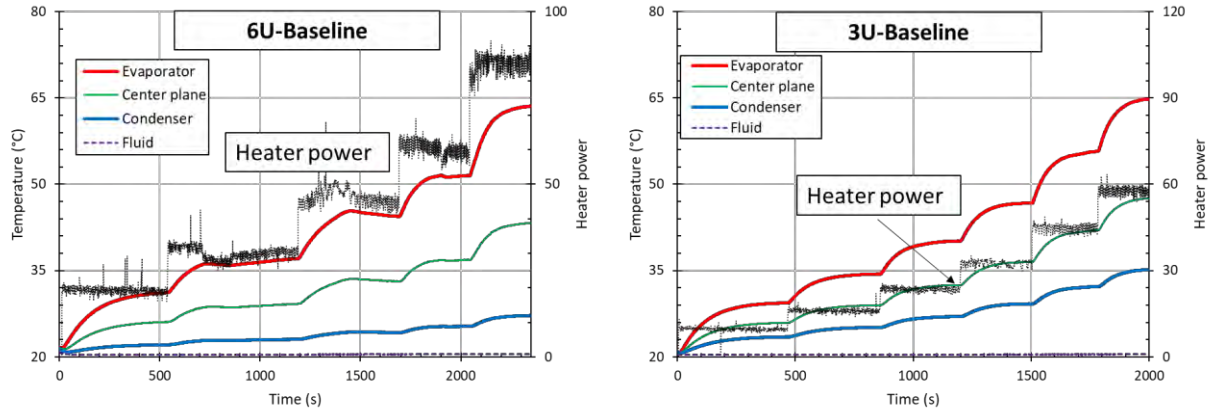

Figure 3. Wall temperature profile of 6U and 3U baseline heat spreaders at 20 °C

Figure 3 shows wall temperature profile of the baseline heat spreader. The wall temperatures increased with increasing heater power. In both heat spreaders, the temperature difference between the evaporator (near

the heat source) and the condenser (neat heat rejection) increased proportional to the heater power. In the 6U heat spreader, the maximum temperature was ~ 64 °C at applied heater power of 85 W. In the case of 3U heat spreader, the maximum temperature was ~ 64.8 °C at 58 W.

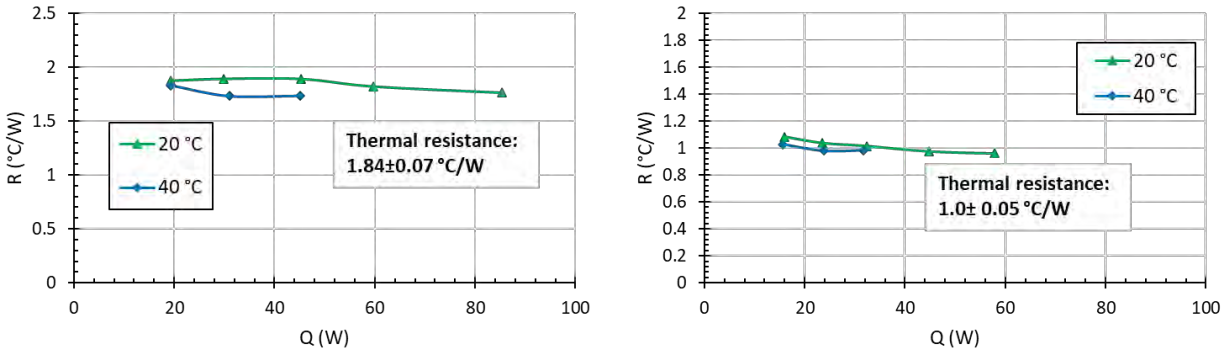

Figure 4. Thermal resistance of the baseline heat spreaders

The thermal resistance of the baseline heat spreaders is shown in Figure 4. The thermal resistance was almost found to be consistent in both cases. The thermal resistance of the baseline 6U heat spreader was 1.84 ± 0.07 °C/W. The thermal resistance of the baseline 3U heat spreader was 1.0±0.05 °C/W. The slight variation in the thermal resistance can be attributed to heat leaks from the heat spreader. At maximum heat spreader temperature of 70 °C and assuming equivalent heat transfer coefficient of 3 W/m^2-K through the insulation, estimated heat leak from the 6U heat spreader was 11.2 W and 4.8 W, respectively.

3.2 Thermal Performance of the 6U form factor EHP and PHP heat spreader

The flat plate type 6U form factor heat spreaders were placed on the test fixture for performance testing at 20 °C and 40 °C operating temperatures.

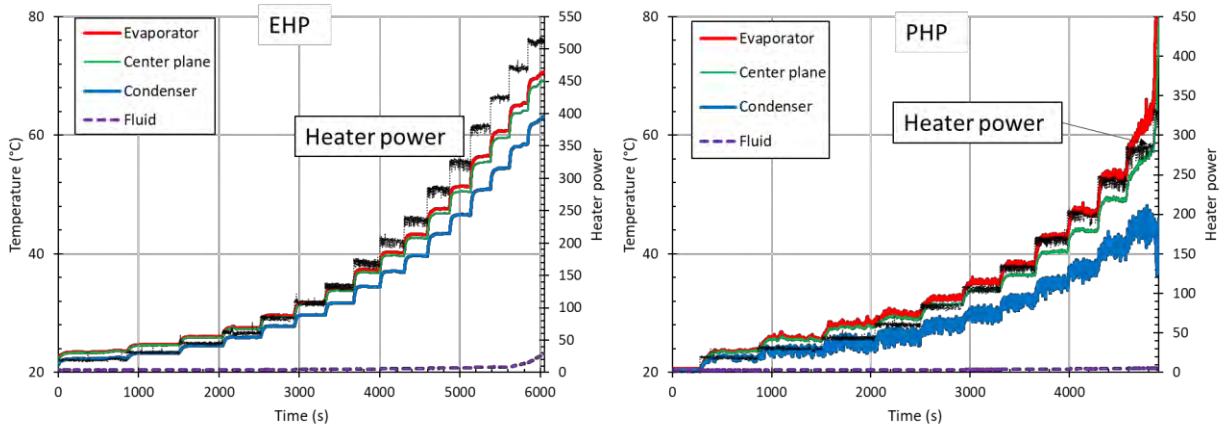

Figure 5. Wall temperature profile of the 6U form factor EHP and PHP heat spreaders at 20 °C operating temperature

Figure 5 shows the temperature profile of the heat spreaders at 20 °C operating temperature. The maximum EHP evaporator temperature was ~69 °C when the applied heater power was ~ 505 W. The EHP did not show any signs of dry-out. On the other hand, the PHP operated until heater power of 238 W, where the maximum temperature was ~ 52.5 °C. As heater power was further increased to 275 W, PHP showed partial dry-out characteristics with greater evaporator-condenser temperature difference. The condenser

temperature still increased in this case. When the heater power was further increased to 325 W, a full dry-out occurred, indicating a sharp increase in the evaporator and decrease in the condenser temperatures.

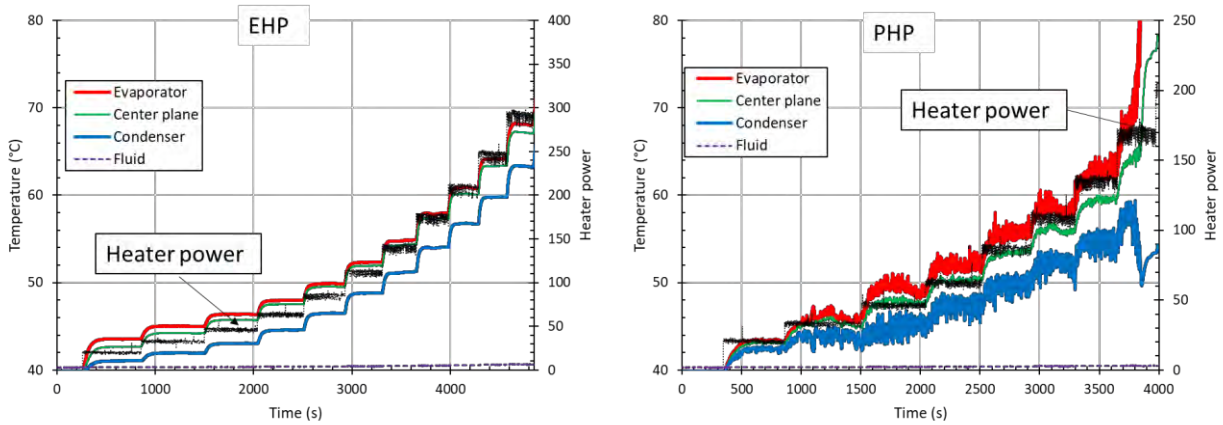

Figure 6. Wall temperature profile of the 6U form factor EHP and PHP heat spreaders at 40 °C operating temperature

Figure 6 shows the temperature profile of the heat spreaders at 40 °C operating temperature. In the EHP, the maximum temperature of 68 °C was observed at 278 W. On the other hand, the at significantly lower power of 135 W, maximum temperature of ~ 64 °C was recorded on the PHP. Further increasing the heater power resulted in dry-out of the PHP. It was observed that the PHP wall temperatures pulsed vigorously indicating temporal dry-out phenomenon, but full dry-out did not occur in the PHP until the heater power of 170 W.

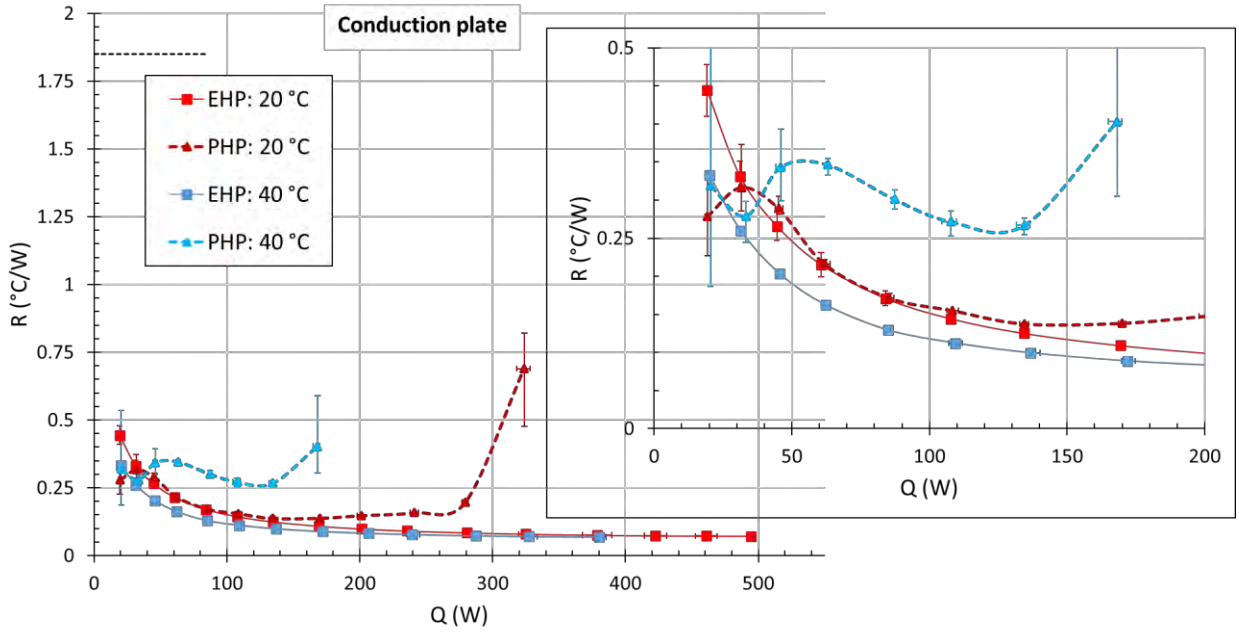

Figure 7. Thermal resistance of the 6U form factor EHP and PHP heat spreaders. The solid line corresponds to the EHP and the dashed line corresponds to the PHP

Figure 7 shows the thermal resistance of the 6U form factor EHP and PHP heat spreaders at varying heat fluxes, for operating heat sink temperatures of 20 °C, and 40 °C. The thermal performance (resistance) of

the heat spreaders was determined in terms of thermal resistance as defined by equation 1. For comparison, the thermal resistance of the baseline plate is shown with a black dotted line. At operating temperature of 20 °C, the thermal resistance of the EHP and the PHP (green lines) were comparable until a heater power of 85 W. At higher heater powers, the PHP showed partial dry-out operation with increasing thermal resistance. The thermal resistance of the EHP, on the other hand decreased, until it plateaued below 0.1 °C/W. In the case of 40 °C sink temperature, the thermal resistance of the EHP was found to be lower than the PHP at all applied heater powers. At applied heater powers below 135 W, the thermal resistance of the PHP was ~ 0.3 °C/W. When heater power increased to 170 W, the PHP showed almost dry-out behavior with vigorously fluctuating, yet increasing wall temperatures until the evaporator temperature was 68 °C, after which, the dry-out occurred in the PHP.

3.3 Thermal Performance of the 3U form factor EHP and PHP heat spreader

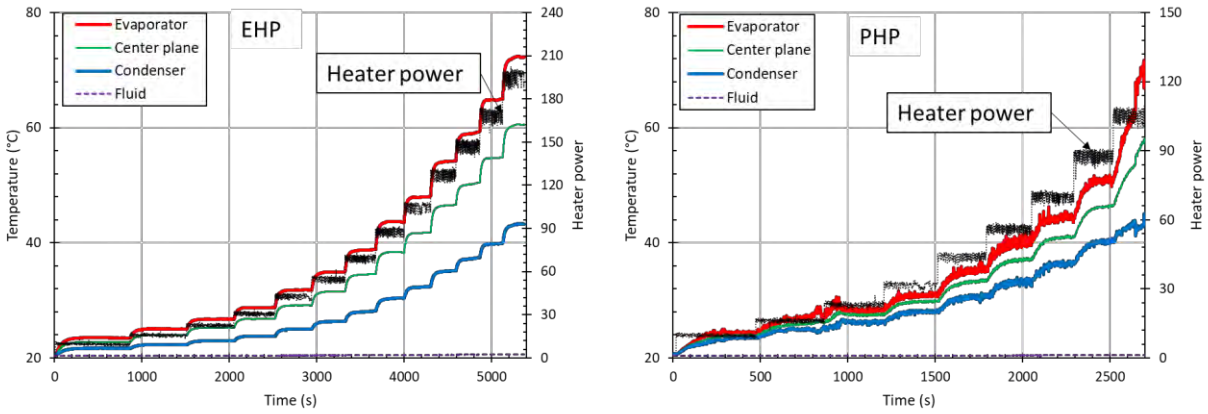

Figure 8. Wall temperature profile of the 3U form factor EHP and PHP heat spreaders at 20 °C operating temperature

Figure 8 shows the wall temperature profile of the 3U EHP and PHP heat spreaders at operating temperature of 20 °C. Maximum EHP temperature of 72.3 °C was recorded at 198 W. On the other hand, the PHP operated until the heater power of 88 W. The evaporator temperature at this point was 51.1 °C. Further increasing the heater power to 104 W led to continuous increase in evaporator-condenser temperature difference showing dry-out. The temperature curves diverged completely when the evaporator temperature surpassed 61.5 °C.

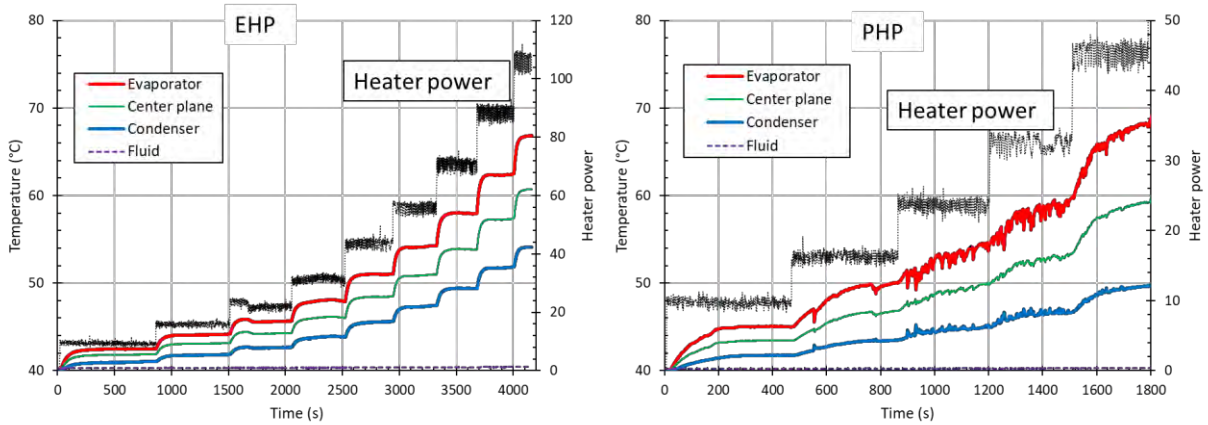

Figure 9. Wall temperature profile of the 3U form factor EHP and PHP heat spreaders at 40 °C operating temperature

Figure 9 shows EHP and PHP wall temperatures at 40 °C operating temperature. Similar to 6U testing, EHP showed normal operation while PHP showed uncharacteristic temperature profile. About 105 W can be transported by the EHP before reaching a maximum temperature of 66.8 °C. On the other hand, the temperature profile of the PHP did not show a steady-state profile after heater power 20 W. However, both evaporator and condenser power increased with increasing power, but with a significantly larger temperature difference compared to the EHP. When the heater power was 45 W, maximum temperature of 68 °C was recorded on the PHP and the testing was stopped.

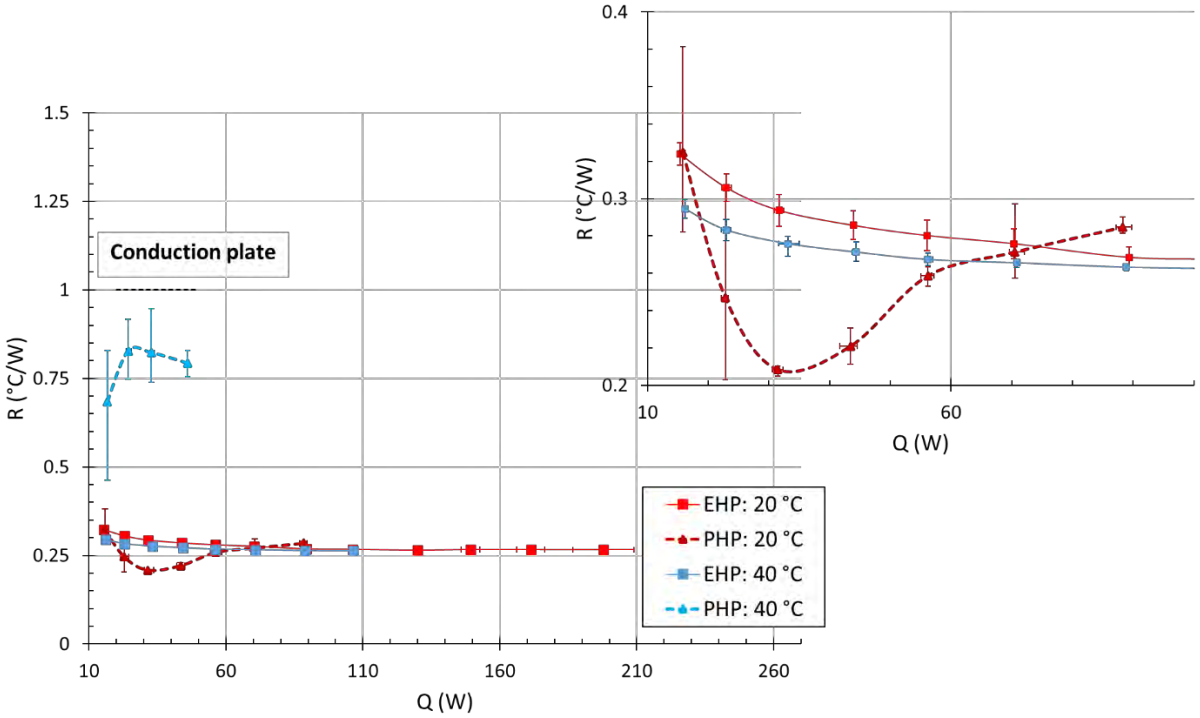

Figure 10. Thermal resistance of the 3U form factor EHP and PHP heat spreaders. The solid line corresponds to the EHP and the dashed line corresponds to the PHP

The thermal performance of the 3U EHP and PHP heat spreaders are Figure 10. When the operating temperature was 20 °C, the thermal resistance of the PHP was lower than the EHP until the heater power was 70 W. The PHP showed lowest thermal resistance of 0.21 °C/W at 30 W, while that of the EHP at that power was 0.29 °C/W. When heater power increased, the thermal resistance trend of the PHP increased, but no dry-out was observed, possibly indicating partial dry-out in the PHP. The EHP operated until the heater power of 198 W without dry-out. At 40 °C operating temperature, the PHP had significantly higher thermal resistance than the EHP, but lower than the baseline. At this operating temperature, the EHP can transport up to 105 W.

It was deduced that propylene is a suitable fluid for PHP and shows good performance for heat spreading at lower operating temperature <20 °C. However, at operating temperatures ≥ 40 °C, the maximum heat transfer limit of the PHP significantly reduces. This can be characterized by either the swept-length limit or the Bond number limit [10, 12]. Swept-length limit is the reduced heat transfer limit of the PHP because the swept-length of the working fluid is smaller than the heated length. This phenomenon occurs in the fluids typically around higher operating temperatures for the chosen working fluid. Bond number limit is the maximum channel diameter for the PHP to maintain liquid slugs. For the chosen diameter of 1.6 mm, the operating temperature corresponding to the Bond number limit is 67 °C. In the 3U PHP at 20 °C operating temperature, the dry-out occurs at around 61.5 °C, indicating that the dry-out phenomenon could

be due to the swept-length limit of the PHP. In all the other cases, the PHP dry-out occurs around 67 °C, indicating that the dry-out likely occurred due to the Bond number limit, but swept-length could also have contributed to dry-out.

5. CONCLUSIONS

Comparative experimental performance EHP and PHP heat spreaders were demonstrated for two different standard electronics form factors-3U and 6U. The EHP is Cu-H_2O heat pipe embedded into an aluminum base plate. The PHP had internal capillary channels for heat transfer by a pulsating two-phase fluid. Propylene was used as the working fluid in the PHP. A central evaporator (1-inch x 1-inch) and two edge condenser configuration was chosen for performance testing. Coolant at a constant temperature was circulated through the heat spreaders. Following conclusions were drawn from the performance testing:

6U heat spreader: At 20 °C operating temperature, the performance of both heat spreaders was comparable until a heater power of 85 W, beyond which EHP showed lower thermal resistance. Dry-out occurred in the PHP when heater power was increased to above 270 W. At 40 °C operating temperature, the thermal resistance of the EHP was lower than the PHP at all heater powers. In the PHP, partial dry-out phenomenon was noted at heater power above 135 W, but full dry-out was not observed since the thermal resistance was significantly lower than the baseline. No dry-out was observed in the EHP.

3U heat spreader: At 20 °C operating temperature, PHP showed lower thermal resistance than the EHP at lower heater powers until 70 W. At higher heater powers, the thermal resistance of the PHP increased indicating partial dry-out phenomenon. At 40 °C operating temperature, EHP demonstrated significantly lower thermal resistance than the PHP.

ACKNOWLEDGMENT

This work was initiated under NASA SBIR Phase I contract #80NSSC21C0211 and is continuing under NASA SBIR Phase II contract #80NSSC22CA205. Additional funding support was obtained under ACT's internal R&D program. Authors are grateful to Dr. Jeffrey R. Didion and Dr. Sergey Semonev for their support as NASA SBIR program technical managers. Authors express their gratitude to engineering Technicians, Mr. Eugene Sweigart, Mr. Justin Boyer, Mr. Samuel Martzall, and Mr. Phil Texter for their support with fabrication and experiments. The authors also thank Mr. Tim Wagner for his support with welding tasks.

NOMENCLATURE

Q	Heater power	(W)	EHP	Embedded heat pipe
R	Thermal resistance	(°C/W)	PHP	Pulsating heat pipe
T	Temperature	(°C)		

References

[1] Y.-G. Lv, W.-X. Chu and Q.-W. Wang, "Thermal management systems for electronics using in deep downhole environment: A review," *International Communications in Heat and Mass Transfer,* vol. 139, p. 106450, 2022.

[2] S. M. S. Murshed and C. A. N. de Castro, "A critical review of traditional and emerging techniques and fluids for electronics cooling," *Renewable and Sustainable Energy Reviews,* vol. 78, pp. 821-833, 2017.

[3] Z. Zhang, X. Wang and Y. Yan, "A review of the state-of-the-art in electronic cooling," *e-Prime - Advances in Electrical Engineering, Electronics and Energy,* vol. 1, p. 100009, 2021.

[4] "Heat Pipes for Thermal Management," Advanced Cooling Technologies, https://www.1-act.com/resources/heat-pipe-resources/faq/#:~:text=What%20is%20a%20Heat%20Pipe,in%20an%20extremely%20efficient%20way..

[5] M. Mameli, M. Marengo and S. Zinna, "Numerical model of a multi-turn Closed Loop Pulsating Heat Pipe: Effects of the local pressure losses due to meanderings," *International Journal of Heat and Mass Transfer,* vol. 55, pp. 1036-1047, 2012.

[6] A. Slippey, W. G. Anderson, M. C. Ellis, C. Hose, J. Schmidt and J. Weyant, "Thermal Management Technologies for Embedded Cooling Applications," in *17th IEEE Intersociety Conference on Thermal and Thermomechanical Phenomena in Electronic Systems (ITherm)*, 2018.

[7] M. T. Ababneh, C. Taru, W. G. Anderson, A. R. A. Hernandez, S. Ortega, J. T. Farmer and R. Hawkins, "Demonstration of Copper-Water Heat Pipes Embedded in High Conductivity (HiK(TM)) Plates in the Advanced Passive Thermal eXperiment (APTX) on the International Space Station," in *48th International Conference on Environmental Systems*, 2018.

[8] H. Yang, S. Khandekar and M. Groll, "Performance characteristics of pulsating heat pipes as integral thermal spreaders," *International Journal of Thermal Sciences,* vol. 48, no. 4, pp. 815-824, 2009.

[9] S. M. Thompson, H. Lu and H. Ma, "Thermal Spreading with Flat-Plate Oscillating Heat Pipes," *Journal of Thermophysics and Heat Transfer,* vol. 29, no. 2, pp. 338-345, 2015.

[10] K.-L. Lee, S. K. Hota, A. Lutz and S. Rokkam, "Advanced Two-Phase Cooling System for Modular Power Electronics," in *51st International Conference on Environmental Systems*, 2022.

[11] A. 48.2-2020, "Mechanical Standard for VPX REDI Conduction Cooling," VITA, 2020.

[12] B. Drolen and C. Smoot, "Performance Limits of Oscillating Heat Pipes: Theory and Validation," *Journal of Thermophysics and Heat Transfer,* vol. 31, no. 4, pp. 920-936, 2017.

[13] K.-L. Lee and S. K. Hota, "Advanced Cooling System for Modular Power Electronics," NASA - SBIR Phase I Report, 2021.